

LEARNING CONTROL AND NEURO-FUZZY LEARNING CONTROL TO INCREASE THE FREQUENCY OF FATIGUE TESTS

Eleazar Cristian Mejía Sánchez, cris_ms@aluno.puc-rio.br

Juan Gerardo Castillo Alva, gcastillo@aluno.puc-rio.br

Marco Antonio Meggiolaro, meggi@puc-rio.br

Jaime Tupiassú Pinho de Castro, jtcastro@puc-rio.br

Pontifical Catholic University of Rio de Janeiro, Rua Marquês de São Vicente 225 Gávea, Rio de Janeiro, RJ, Brazil

Timothy Hamilton Topper, topper@waterloo.ca

University of Waterloo, 200 University Avenue West, Waterloo, Ontario, Canada

Abstract. In this paper, learning control and neuro-fuzzy learning control techniques are developed and applied to material testing machines, allowing the application of variable amplitude loads at high frequencies. The proposed methodology consists in implementing a bang-bang control type to restrict the servo-valve system to permanently work at its extreme operation limits, always completely open in either one or the other direction. The inputs for both algorithms are the range (twice the amplitude) and minimum component of each load event to be applied to the test specimen. Both the learning algorithm and the neuro-fuzzy learning algorithm try to obtain the optimal instants for the servo-valve reversions, associating them to a non-dimensional variable with values between 0 and 1. The learning algorithm makes use of a table to store the non-dimensional variables associated with each range-minimum combination. The table values are constantly updated by the learning laws during the test execution, improving the system response. The neuro-fuzzy techniques, on the other hand, do not need such tables, which decreases the memory requirements of the computational system. The range and minimum values of each loading event are entered in the neuro-fuzzy system, which then calculates the instant of reversion of the servo-valve. The learning process is done by updating the weights of the neuro-fuzzy system, based on the measured errors during the tests, gradually improving the system response. The validation of the proposed methods is made using a servo-hydraulic testing machine with a 100kN capacity. The control methods are implemented in real time control software running in a CompactRio computational system. Experimental results show that the test frequency can be significantly increased with the proposed control techniques, even for variable amplitude load histories.

Keywords: Learning control; bang-bang control; neuro-fuzzy learning control.

1. INTRODUCTION

Hydraulic systems are widely used in industrial systems in applications such as automated plants, robotics, motion simulators, metal processing plants, mineral exploration, presses, heavy machinery and materials fatigue test systems (Merritt, 1967). In general, hydraulic systems are used in applications where relatively high forces, torques and accelerations are required. Machinery used in materials fatigue testing is based on servo-hydraulic systems, to provide useful information about the material's life in service by applying load cycles. The applied load may be repeated millions of times in typical frequencies up to one hundred times per second for metals. To achieve these frequencies, relatively high in a typical fatigue test, it is necessary to have an efficient control system.

In traditional control methods, all information from the process is known in advance, deterministically described (Doebelin, 1976). If the initial information is unknown, a controller may be designed to estimate the information during the operation. This information could be used for future control decisions, a process known as learning control. The literature related to the control of servo-hydraulic systems presents many developments applied to industrial manipulators used to perform repetitive tasks (Sun and Chiu, 1999). One of these works is based on a Lyapunov controller, where the adaptive law is also proposed to remove uncertainties in the hydraulic parameters (Soroushpour and Salcudean, 2000). A second work uses a non-linear controller that presents a better performance in both simulations and experiments than the results obtained using the proportional-derivative controller (Jelali and Krol, 2003). Another work uses a robust controller and disturbance rejection for servo-hydraulic systems (Ching Lu and Wen Chen , 1993). In this case, the results of simulations and experiments show that this controller has the ability to maintain the load accuracy in the presence of very large variations of the plant parameters and/or external disturbances.

Over the last years, system based in Neural Networks and Fuzzy were finding a way in control applications and many other areas of engineering. A scheme of control by neural Networks does not required the computation of the non-linear dynamic of manipulators, only use signs measured locally to make the learning of the behavior of the system by updating the weights of the network that minimize the error between the real and the desired output. The results captured the attention of engineers working with real systems. This is due, mainly to the results obtained and often the ease of implementation when develop control systems based on neural networks and fuzzy by Lewis et al., (2002).

Another work presented the use of a learning control, using Neuro-Fuzzy techniques to design the trajectory control using an electro-hydraulic actuator (Branco and Dente, 1998). Another application uses a Adaptive Neuro-Fuzzy Model Reference Control (ANFMRC), developed to improve control performance in a pneumatic system, this hybrid control is combined with a “bang-bang” applied when the error is high, and a ANFMRC is applied when the error is small (Kaitwanidvilai and Parnishkun, 2004).

In the present work, Learning Control and Neuro-Fuzzy Learning Control are developed to increase the frequency of the applied load cycles in fatigue tests. An experimental control system is developed and applied to a fatigue test machine in order to assess and evaluate the performance of the proposed methodology.

2. LEARNING CONTROL

The learning process can be seen as a problem of estimation or successive approximations of unknown quantities or unknown function (King-Sun, 1970). In this case, the unknown quantities that are estimated or learned by the controller are parameters that are governed by the control laws.

The block diagram shown in Figure 1 represents the learning control process. In each cycle, the system uses the information of the variables U_{II} stored in its memory for feedback control. The errors measured at each cycle are used to update the parameters U_{II} through a learning law. The learning law is applied only at the end of each learning cycle k , which updates the values $U_{II}(k)$ with $U_{II}(k+1)$ based on the errors $e(k)$. In the present application in fatigue testing, each learning cycle is associated with each reversal of the controlled parameter, e.g., after one peak and one valley of the applied force history.

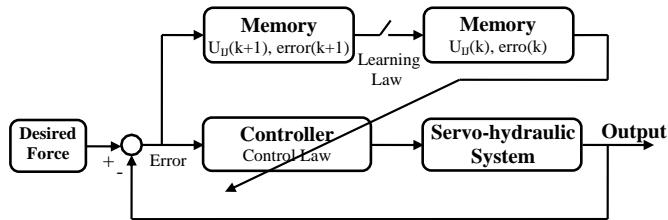


Figure 1: Block diagram of the learning control

The learning control methodology presented in this work aims to maintain the servo-valve working in its extreme operation limits, keeping the valve most of the time in the fully open position in either direction. This type of control is known as bang-bang (O’ Brien, 2006). Due to the system dynamics, the servo-valve reversion instants must be chosen to happen before the desired peaks and valleys of force or stress.

This instant of reversion is represented by a non-dimensional variable U_{II} , which is defined as the fraction of the peak-valley (or valley-peak) path where the valve should be reverted. For instance, when controlling a force cycle from 10 to 110kN, a value $U_{II} = 0.8$ would be equivalent to reversing the valve when 80% of the path between 10 and 110kN has passed, i.e., when the measured force is equal to $10 + 0.8 \times (110 - 10) = 90. In this same example, when returning from 110 to 10kN, the same value $U_{II} = 0.8$ would be equivalent to reversing the valve at $110 - 0.8 \times (110 - 10) = 30.$$

This U_{II} is a parameter that depends on several factors such as the amplitude and mean value of the applied load, and it is also influenced by dead zones caused in some cases by slacks in the test specimen fixtures. The objective of the proposed approach is to learn the values of U_{II} as a function of the load amplitude, mean, and direction (either from peak to valley or from valley to peak), as described next.

2.1 Learning tables

Figure 2 shows a table that stores non-dimensional numbers U_{ij} (with the indexes in lower-case) associated with the learning process. These numbers are the discrete values of U_{II} for several combinations of load amplitude and mean. The columns show the values of the gamma (or range, equal to twice the amplitude) of the physical variable to be controlled, while the rows show the minimum value of the peak-valley half-cycle. Note that this table can be divided into two parts, one associated to when the system is going from a valley to a peak, and another when it is going from a peak to a valley. In order to join both tables, the concept of negative gamma is used, which indicates the transition from a peak to a valley.

		Coluns (gamma)					
		-25	-15	-5	5	15	25
Lines (minimum)	-25	0,9810	0,9602	0,8795	0,8016	0,8712	0,9475
	-15	0,9688	0,9415	U_{ij}	0,8245	0,9005	0,9516
	-5	0,9520	0,9230	0,8456	0,8429	0,9406	0,9712
	15	0,9256	0,8910	0,7415	0,9038	0,9668	0,9856
	25	0,9086	0,8723	0,6879	0,9312	0,9765	0,9901

Figure 2: Learning table

As a result, U_{ij} is defined as an element associated with the row i (minimum value “ min_i ”) and the column j (associated with the gamma “ $gama_j$ ”). For a loading with a minimum value min_i and gamma equal to $gama_j$, then $U_{II} = U_{ij}$. If the minimum and gamma values are between two consecutive values in the table, i.e., $min_i < min < min_{i+1}$ and $gama_j < gama < gama_{j+1}$, then U_{II} is obtained from an interpolation (see Figure 3):

$$U_{II} = a + (b - a) \cdot \frac{(gama - gama_j)}{(gama_{j+1} - gama_j)} \quad (1)$$

where

$$a = U_{i,j} + (U_{i+1,j} - U_{i,j}) \cdot \frac{(min - min_i)}{(min_{i+1} - min_i)} \quad (2)$$

$$b = U_{i,j+1} + (U_{i+1,j+1} - U_{i,j+1}) \cdot \frac{(min - min_i)}{(min_{i+1} - min_i)} \quad (3)$$

			gama _j	gama _{j+1}	
	0,8595	0,8364	0,8153	0,9314	0,9650
min _i	0,8143	0,7923	U_{ij}	U_{i,j+1}	0,9736
min _{i+1}	0,7640	0,7289	U_{i+1,j}	U_{i+1,j+1}	0,9812
	0,7128	0,6935	0,9216	0,9715	0,9878
	0,6550	0,6320	0,9418	0,9835	0,9934

Figure 3: Procedure for interpolation when the values of gamma and minimum are between two cells

Once the value of U_{II} is calculated from Eqs. (1-3), the servo-valve reversal point can be calculated from

$$reversal = \begin{cases} min + U_{II} \cdot gama & \text{(from valley to peak)} \\ (min + gama) - U_{II} \cdot gama & \text{(from peak to valley)} \end{cases} \quad (4)$$

2.2 Learning Law

The learning law governs how the $U_{i,j}$ values are updated after each load reversion in the test. Thus, the new value of $U_{i,j}$ is calculated using the error between the measured peak (or valley) x and the desired peak (or valley) x_d :

$$e = \frac{x_d - x}{x_d - x'} \quad (5)$$

where x' is the valley or peak measured in the last reversion. Note that the defined error is dimensionless, and that x can be any variable to be controlled in the tests, such as applied force, test specimen deformation, or hydraulic piston displacement.

In the case where x and x_d are peaks, x' will be a valley, and the difference $(x_d - x')$ will be positive. Thus, if there is an undershoot in this event, then $x < x_d$, resulting in $e > 0$. Analogously, if an overshoot happens, then $e < 0$. On the other hand, if x and x_d are valleys, then x' will be a peak, and the difference $(x_d - x')$ will be negative. In the case of an undershoot when the loading decreases, then $x > x_d$, and therefore $e > 0$. Similarly, for an overshoot, $e < 0$.

As a result, positive errors are always associated to undershoots, while negative ones to overshoots, no matter if the transition is from a valley to a peak or from a peak to a valley. Clearly, if an overshoot happens, then the approach is to reverse the valve sooner in future similar events, which implies in decreasing $U_{i,j}$ for that combination of (*min, gamma*). On the other hand, in the case of an undershoot, it would be necessary to increase $U_{i,j}$.

Assuming that any undershoot or overshoot will remain below 100%, then $-1 < e < 1$, and a learning law can be proposed:

$$U_{i,j} := U_{i,j} \cdot (1 + e) \quad (6)$$

The above learning law does not need adjustable gains. It is associated with an increment of $U_{i,j}$ by a factor $(1+e)$ in the case of an undershoot ($e > 0$), and a decrease in its value for an overshoot ($e < 0$). It is possible to introduce a gain to multiply the error in equation (6), in order to tune the learning rate. Nevertheless, a unitary gain was enough in this work to achieve a stable and fast learning law.

Since the learning table only stores discrete values of $U_{i,j}$, the values $U_{i,j}, U_{i,j+1}, U_{i+1,j}, U_{i+1,j+1}$ that generated $U_{i,j}$ (*min, gamma*) by interpolation must also be updated according to the learning law, where $\min_i < \min < \min_{i+1}$ and also $\gamma_{i,j} < \gamma < \gamma_{i+1,j+1}$. This update process is also made using weight factors, i.e., the neighboring cell closer to $U_{i,j}$ shall be updated in a greater degree than the other three neighbor cells. This process is easily implemented with the learning law:

$$U_{i,j} := U_{i,j} \cdot [1 + (1 - \alpha) \cdot (1 - \beta) \cdot e] \quad (7)$$

$$U_{i,j+1} := U_{i,j+1} \cdot [1 + (1 - \alpha) \cdot \beta \cdot e] \quad (8)$$

$$U_{i+1,j} := U_{i+1,j} \cdot [1 + \alpha \cdot (1 - \beta) \cdot e] \quad (9)$$

$$U_{i+1,j+1} := U_{i+1,j+1} \cdot [1 + \alpha \cdot \beta \cdot e] \quad (10)$$

where

$$\alpha = \frac{\min - \min_i}{\min_{i+1} - \min_i}, \quad 0 < \alpha < 1 \quad (11)$$

$$\beta = \frac{\gamma - \gamma_{i,j}}{\gamma_{i+1,j+1} - \gamma_{i,j}}, \quad 0 < \beta < 1 \quad (12)$$

Note that Eqs. (1-3) may be rewritten in terms of the above defined α and β as follows:

$$U_{i,j} := U_{i,j} \cdot (1 - \alpha) \cdot (1 - \beta) + U_{i+1,j} \cdot \alpha \cdot (1 - \beta) + U_{i,j+1} \cdot (1 - \alpha) \cdot \beta + U_{i+1,j+1} \cdot \alpha \cdot \beta \quad (13)$$

3. NEURO-FUZZY LEARNING CONTROL

In this control model, the unknown information is estimated or learned by the Neuro-Fuzzy system and provided to the bang-bang control. Thus, as the Neuro-Fuzzy system stores more information, the controller is upgraded by improving system performance.

Figure 4 shows the block diagram that illustrates the Neuro-Fuzzy learning control. In this control model, the information is represented by the same U_{II} variable described above, and in that case it is the output of Neuro-Fuzzy system. The information that generates the U_{II} value is stored in the weights of the Neuro-Fuzzy system structure. The U_{II} variable used to change the control action on the servo valve is updated after each cycle of operation by adjusting the weights of Neuro-Fuzzy structure using a learning algorithm based on the measured errors.

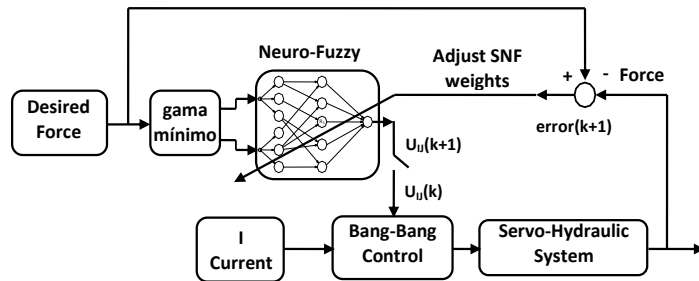


Figure 4: Block diagram of the Neuro-Fuzzy learning control

3.1 Neuro-Fuzzy System

The inputs of the Neuro-Fuzzy systems are the “*gama*” and “*minimo*” variables of controlled magnitude, while the output is the U_{II} variable. The Neuro-Fuzzy system consists of two hidden layers: the Neuro-Fuzzy and the rules layer. The Neuro-Fuzzy weights ω_{ij} between the rules and the output layers are updated using the backpropagation learning algorithm based on error($k+1$) to each iteration (see Figure 5).

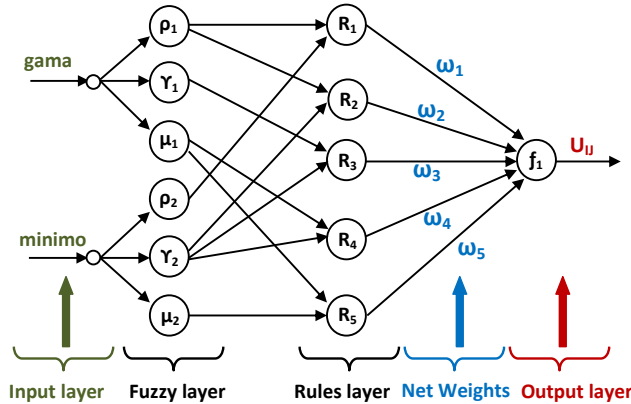


Figure 5: Neuro-Fuzzy System Structure

3.2 Neuro-Fuzzy Modeling

The learning control based on a hybrid Neuro-Fuzzy System (NFS) is usually formed by the combination of fuzzy systems and Artificial Neural Networks (ANN). It combines the advantages of ANN such as learning ability, optimization, and the connection structure with the advantages of fuzzy systems, which uses reasoning similar to human, with proficiency to add information from experts.

The modeling of this system is determined by the settings of the characteristics of their "parents", the Fuzzy and Neural parts (see Figure 6).

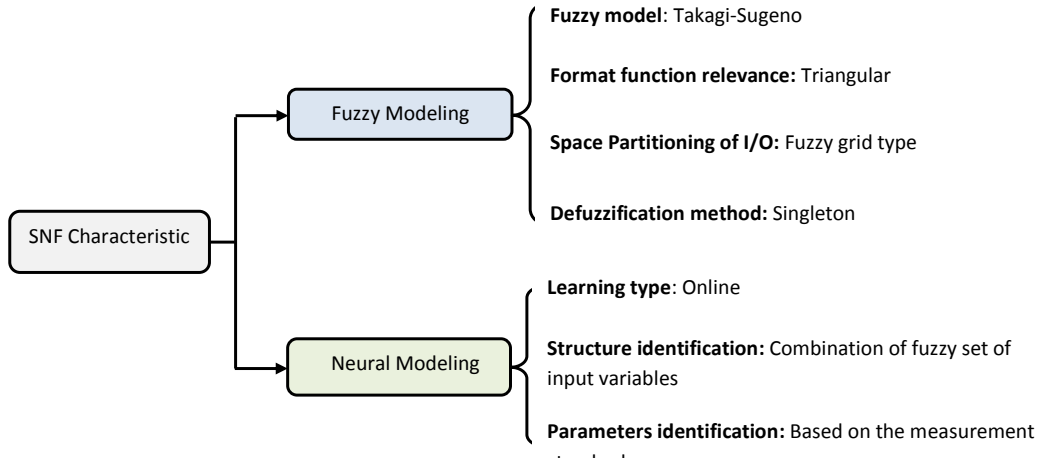


Figure 6: Neuro-Fuzzy Modeling

3.3 Neuro-Fuzzy Learning Control

U_{IJ} Value Calculation

The U_{IJ} value of the dimensionless variable is obtained as the result of NFS evaluation for each combination of minimum and gamma values. Thus, for load with a minimum value equal to min_i , and gamma value equal $gama_j$, U_{IJ} is the NFS output. The gamma values are positive when the system is going from a valley to a peak. These entries variables of NFS (minimum and gamma) are normalized in the range [-1, 1] using the following equation:

$$x_n = \frac{2.(x - \min)}{\text{Max} - \min} - 1 \quad (14)$$

where x_n is the normalized value of the variable x, min and Max are the minimum and maximum values of the variable x.

The normalization of minimum and gamma input variables is done by using the following equation:

$$\min_n = \frac{\min}{100} \quad (15)$$

$$gama_n = \frac{gama}{200} \quad (16)$$

where 100 kN is the minim value of the minimum variable and 200 kN is the maximum value of the gamma variable.

After normalization of the input variables in the input layer, see Figure 7, the fuzzy layer is calculated by the relevance degree that the entries satisfy the fuzzy sets associated with each entry.

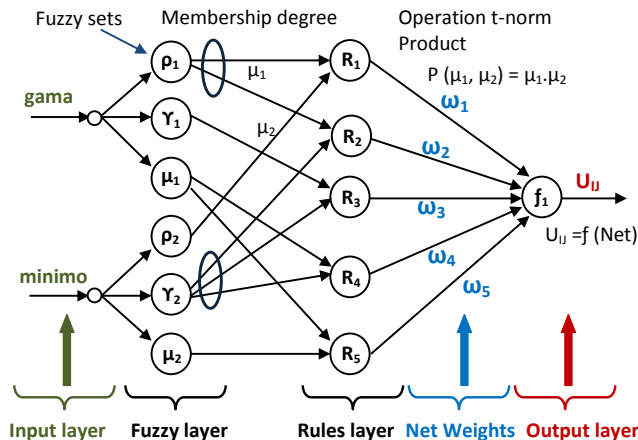


Figure 7: U_{IJ} estimation and description of NFS layers.

In the rules layer, the trigger level corresponding to each rule is calculated, performing the t-norm (product) operation

$$P_k(\mu_i, \mu_j) = \mu_i \cdot \mu_j \quad (17)$$

In the output layer, the U_{II} value is calculated as a function of $P_k(\mu_i, \mu_j)$ and ω_k :

$$U_{II} = f(Net)$$

$$Net = \frac{\sum_{k=1}^M P_k(\mu_i, \mu_j) \cdot \omega_k}{\sum_{k=1}^M P_k(\mu_i, \mu_j)} \quad (18)$$

In this work, f is considered as the linear activation function, so

$$U_{II} = \frac{\sum_{k=1}^M P_k(\mu_i, \mu_j) \cdot \omega_k}{\sum_{k=1}^M P_k(\mu_i, \mu_j)} \quad (19)$$

where $P_k(\mu_i, \mu_j)$ is the result of the *t-norm* operation in the rules layer, and ω_k is the connection weight of the rule k . The calculated U_{II} value and the servo-valve reversal points are calculated from the Eq. (4).

Learning Law of NFS

The learning of the NFS is made by the update of ω_k weights in the following instant with the current value. All ω_k values are initialized with a fixed value, and then they are updated according to the standard error, the learning rate and the activation level of each rule. The normalized error is calculated by Eq. (5).

Usually, the error value is in the range $[-1, 1]$ and the algorithm of updating ω_k NFS weights is given by the following learning law:

$$\omega_k(t+1) = \omega_k(t) + \Delta\omega_k(t) \quad (20)$$

$$\Delta\omega_k(t) = \eta \cdot e \cdot \frac{P_k(\mu_i, \mu_j)}{\max[P_k(\mu_i, \mu_j)]} \quad (21)$$

where $\omega_k(t)$ is the connection weight corresponding to the rule k , η is the learning rate, e is the normalized error, and $P_k(\mu_i, \mu_j)$ is the trigger level corresponding to the rule k .

4. EXPERIMENTAL SYSTEM

The proposed methodology is applied to a fatigue test machine INSTRON model 8501, with a servo-valve MOOG D562 and a current signal command of ± 40 mA.

The piston from this machine can generate forces up to 100 kN with a displacement amplitude of ± 50 mm (from a central position). The fatigue test machine has a force sensor (load cell) to control force histories, and a LVDT for displacement commands. A strain-gage or clip-gage attached to the test specimen also allows the control of a deformation history. The hydraulic fluid is supplied by a hydraulic pump at the pressure of 190 bar.

The learning control is implemented in a CompactRIO cRIO9004 computational system, from National Instruments. This system includes modules for analog outputs (NI9263), analog inputs, exciter module for strain gages (NI9237), and a voltage-to-current converter, see Figure 8.

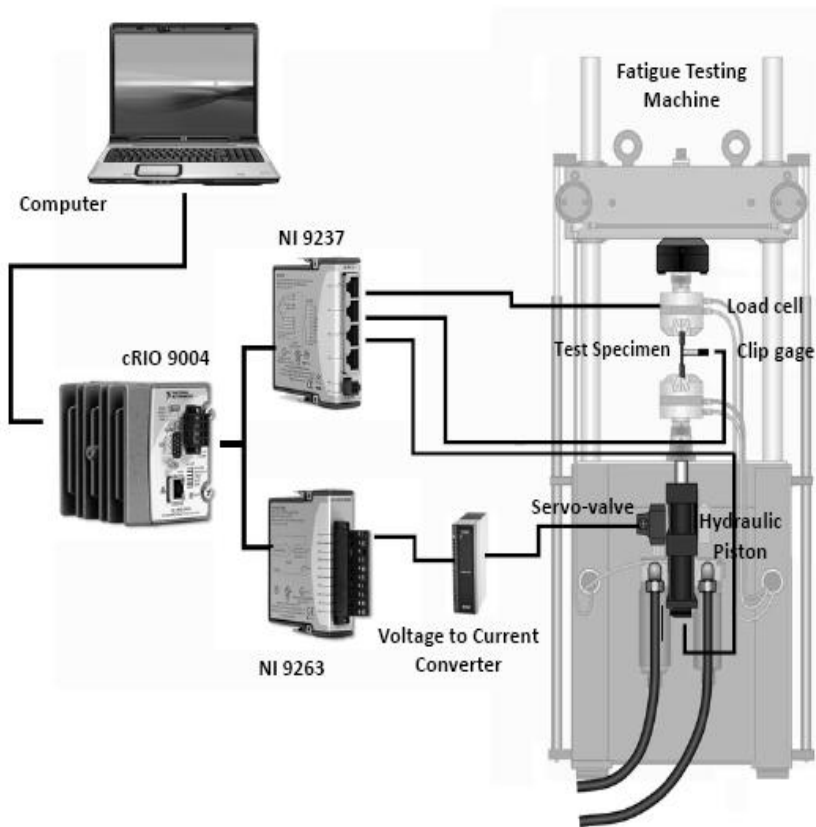


Figure 8: Experimental System

The software was developed using LabVIEW8.0 to perform the tests on the experimental system described above, which includes acting on the system and reading data. The user can visualize in real time the errors, the U_{IJ} values, desired load peaks and valleys, reached peaks and valleys, as well as force, position and stress values.

5. SIMULATIONS

Simulations of the proposed control system applied to a servo-hydraulic testing machine are performed in MATLABTM. The simulation includes the modeling of a 100kN servo-hydraulic machine, including detailed models for the servo-valve (Viersma, 1980), (Thayer, 1965). The system model is too lengthy to be included in this work; however, its full description can be seen in Alva (2008).

5.1 Learning Control Simulations

The simulations for the servo-hydraulic machine, performed for constant and variable amplitude load histories, show satisfactory results for the proposed learning control law. Figures 9 shows how the controller learns by changing the location of the servo-valve reversion points (represented by an “x”) at each load cycle. The learning process starts assuming U_{IJ} equal to 0.5 for any value of (\min, \max).

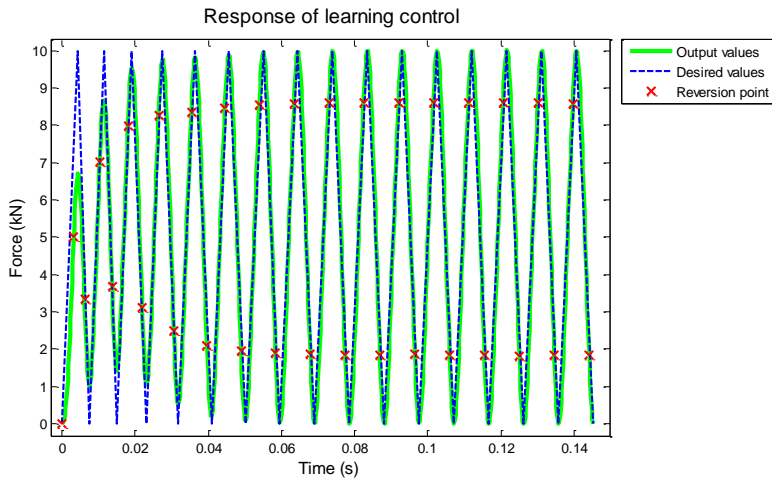


Figure 9: Learning control response for a constant amplitude history ranging from 0 to 10kN.

As shown in Fig. 10, the learning process also presents good results for variable amplitude histories. In this example, three blocks with different (*min*, *gama*) values need to be applied to the specimen. In the first block, the learning process takes about 5 to 6 cycles to converge. The second block also needs 6 blocks to converge, because its (*min*, *gama*) is very different from the one from the first block, updating a very different section of the learning table. But the learning in the third block converges in only 2 cycles, because it could benefit from the updated U_{ij} values learned from the second block, which had similar (*min*, *gama*) values.

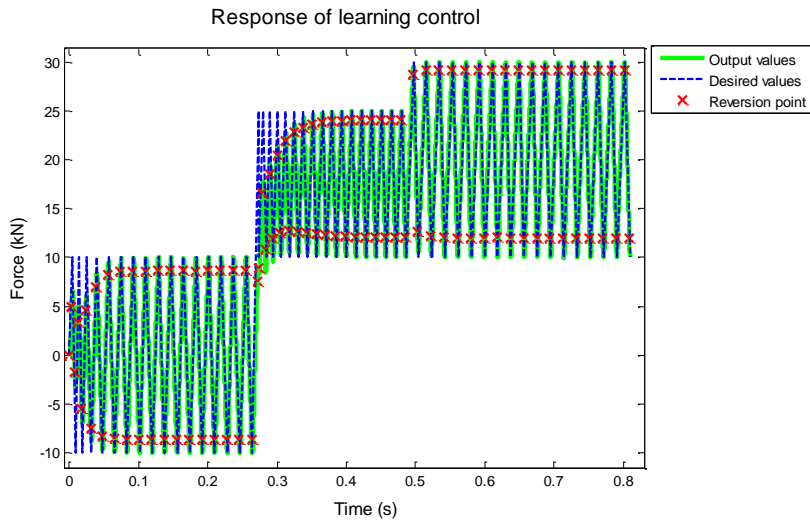


Figure 10: Learning control responses for a variable amplitude input.

Note also from Fig. 10 that the frequency of the system response depends on the desired amplitude. The blocks 1 and 3, which have the same amplitude $[10 - (-10)]/2 = [30 - 10]/2 = 10$ kN, result in a higher frequency than block 2, with a lower amplitude $[25 - 10]/2 = 7.5$ kN. This variable frequency is not an issue in fatigue testing, because the fatigue life of most materials under room temperature depends only on the load amplitude and mean, not on its frequency. These frequencies, on the other hand, are the highest achievable for a given system and load history, since the servo-valves are always operating at their operational limits and their reversion has been optimized due to the learning law.

5.2 Neuro-Fuzzy Learning Control Simulations

Figure 11 shows the simulations for constant amplitude loads ranging between ± 10 kN, with a learning rate $\eta = 0.95$. The peak/valley reversal points are modified as new loadings are presented by converging on an optimal reversal value. Therefore, in future loadings with same amplitude, the controller can respond satisfactorily without the need for learning again. The satisfactory behavior is also observed in Figure 12, for variable amplitude loading.

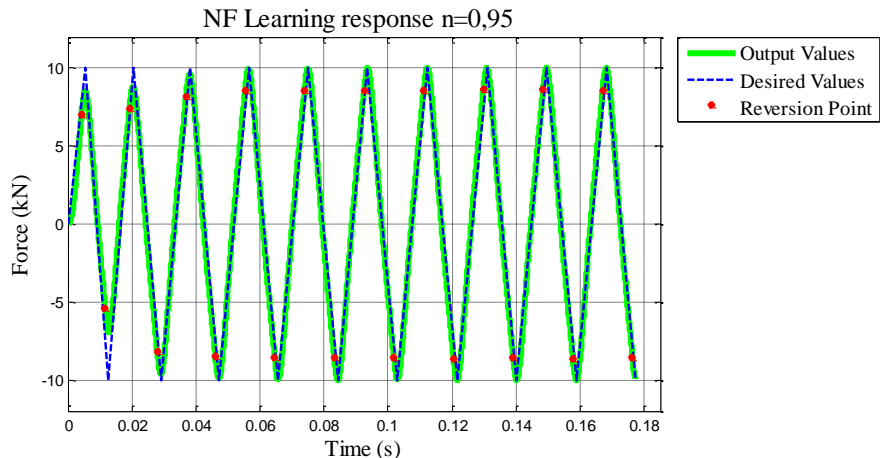


Figure 11: Neuro-Fuzzy Learning control response for a constant amplitude loading.

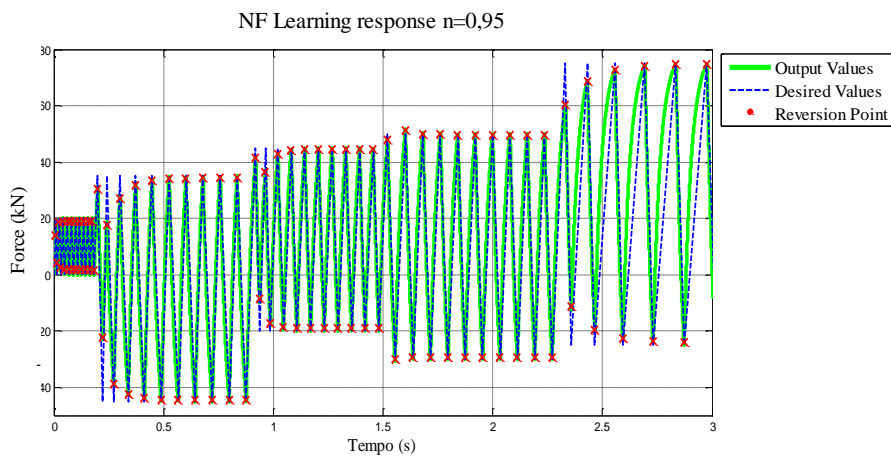


Figure 12: Neuro-Fuzzy Learning control responses for a variable amplitude input.

5.3 Comparison between Control Models

The convergence to zero of the force control error during the learning process is shown in Figure 13, for the same loading history. It may be observed that the Neuro-Fuzzy learning control has a faster convergence rate, with a higher learning speed.

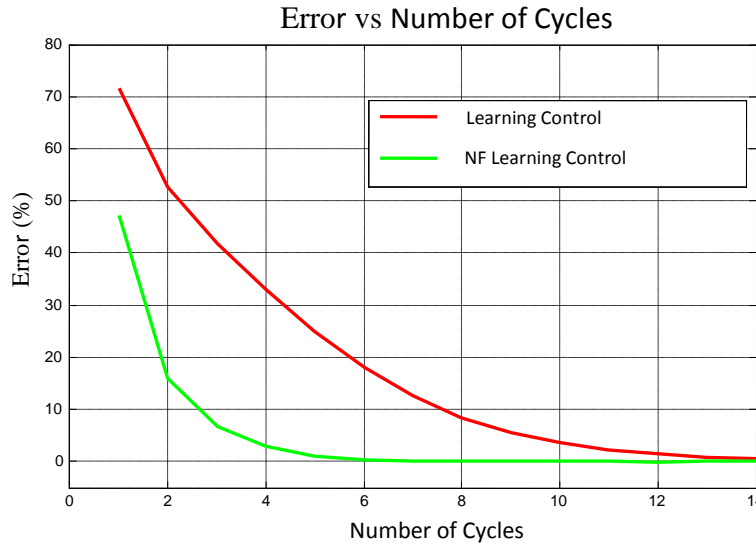


Figure 13: Performance of learning control models for $\pm 25\text{kN}$ of constant load

Figure 14, shows the number of cycles until the control can achieve an error smaller than a permissible value, in this case defined by 2% (98% accuracy), depending on the learning rate for a load of $\pm 25\text{ kN}$. The Neuro-Fuzzy learning control has a more faster than the learning control.

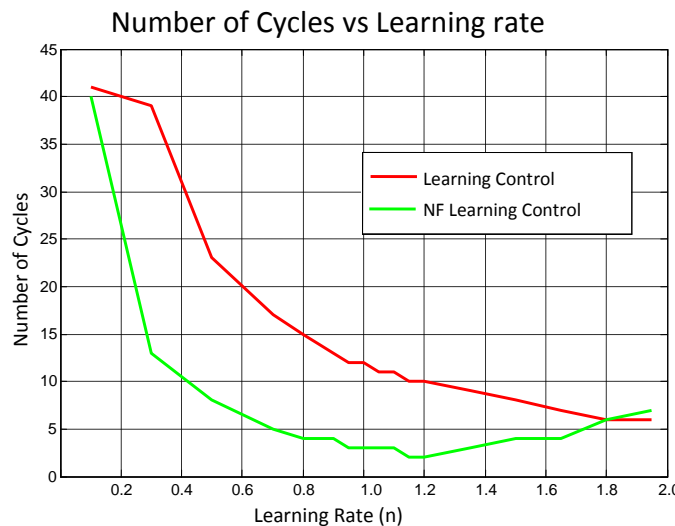


Figure 14: Number of cycles of convergence as a function of the learning rate, for a $\pm 25\text{ kN}$ loading.

6. EXPERIMENTAL RESULTS

Experiments are performed for loading histories with zero mean and with force amplitudes of 10 kN, 20 kN, 30 kN and 40 kN, all of them using $\pm 20\text{mA}$ for the maximum servo-valve current. The tests are performed using εN steel test specimens with 12mm in diameter in its thinnest section.

Figure 15 compares the performance of the proposed learning and NF learning controls with the standard control used by Instron. The Neuro-Fuzzy learning control and the learning control were implemented using lower $\pm 20\text{mA}$ servo-valve current limits, instead of the $\pm 40\text{mA}$ limits from the Instron controller hardware, under several load amplitudes. It is possible to observe a better performance of the learning control and the Neuro-Fuzzy learning control for low amplitudes and a similar performance for high amplitudes over the Instron controller at $\pm 40\text{mA}$, only needing

half the current to operate the servo-valve. The traditional Instron control is only able to outcome the proposed controls when it is allowed to use currents beyond 40mA in the servo-valve (overdrive mode).

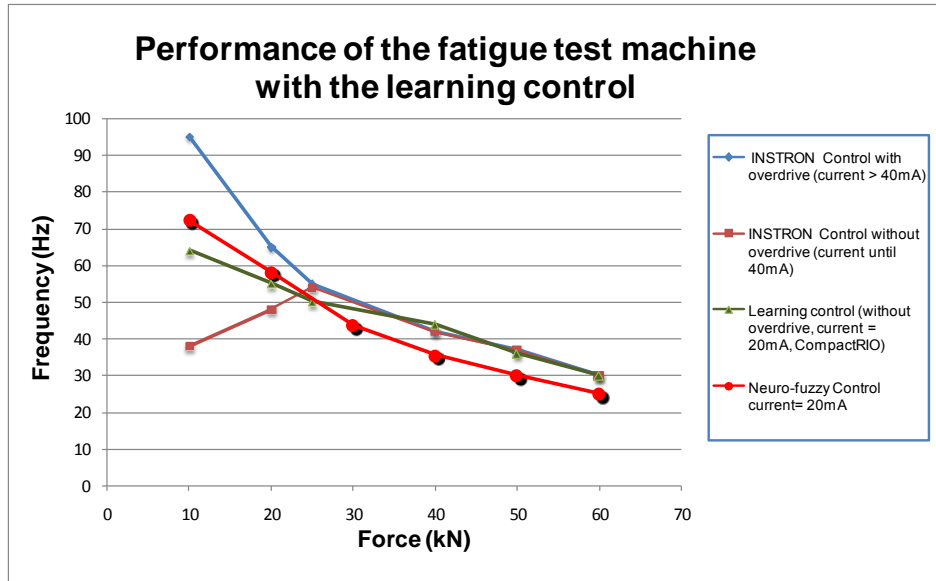


Figure 15: Performance of the fatigue test machine.

7. CONCLUSIONS

In this work, it was shown that it is possible to increase the work frequency of a fatigue test machine using a learning control technique and a Neuro-Fuzzy learning control applied to servo-hydraulic systems. The difference between the learning control and the Neuro-Fuzzy learning control is that the latter does not need the use of large tables to store the tuned parameters because all the updates of the learning process are stored in the weights of Neuro-Fuzzy system. This model presents a better performance in simulations for both constant and variable amplitude loading, with low memory requirements. Both control models do not need user-defined adjustable gains, simplifying their implementation. The proposed control systems were simulated and applied to a fatigue testing machine, implemented in a CompactRIO computational system. The results showed that the proposed controls were capable to generate frequencies higher than those obtained with the original controller, even when using lower current limits for the servo-valve triggering.

8. REFERENCES

- Alva J.G.C., “Controle por Aprendizado de Sistemas Servo-Hidráulicos de Alta Frequência,” M.Sc. Dissertation, Pontifical Catholic University of Rio de Janeiro, in Portuguese, 2008.
- Branco, P. J.; Dente, J. A. “Design of an Electro-Hydraulic System Using Neuro-Fuzzy Techniques”. Mechatronics Laboratory. Department of Electrical and Computer Engineering. Instituto Superior Técnico, Lisboa. Portugal – 1998. pp. 190-206.
- Ching Lu H., Wen Chen L., “Robust Controller with Disturbance Rejection for Hydraulic Servo Systems,” IEEE Transactions on Industrial Electronics, vol. 40, pp. 152-162, 1993.
- Doebelin, E.O., “System Dynamics: System Modeling and response”. Prentice Hall, 1976.
- Jelali M., Kroll A., “Hydraulic servo-systems: modeling, identification and control”. New York. Springer, 2003.
- Kaitwanidvilai, S.; Parnishkun, M. “Force Control in a Pneumatic System using Hibrid Adaptive Neuro-Fuzzy Model Reference Control”. School of Advanced Technologies, Asian Institute of Technology. Thailand – 2004. pp. 23-41.
- King-Sun F., “Learning Control System,” IEEE Transactions on Automatic Control, pp. 210-221, 1970.
- Lewis, F. L.; Campos, J. e Selmic, R. “Neuro-Fuzzy Control of industrial System with Actuator Nonlinearities”. Philadelphia, 2002.
- Merritt H.E., “Hydraulic Control Systems”. John Wiley and Sons, 1967.
- O’ Brien R.T., “Bang Bang Control for Type-2 Systems,” 38th Southeastern Symposium System Theory, Tennessee, USA, 2006.
- Sirouspour M., Salcudean S., “On the Nonlinear Control of Hydraulic Servo-Systems,” IEEE International Conference on Robotics and Automation, San Francisco, 2000.
- Sun H., Chiu G., “Nonlinear Observer Based Force Control of Electro Hydraulic Actuators,” American Control Conference. San Diego, CA, USA, 1999.
- Thayer W.J., “Transfer Functions for MOOG Servovalves,” Technical Bulletin. New York, NY, USA, 1965.
- Viersma T.J., Analysis, Synthesis and Design of Hydraulic Servosystems and Pipelines. Elsevier, 1980.

9. RESPONSIBILITY NOTICE

The authors are the only responsible for the printed material included in this paper.